ISSN 0020-1685, Inorganic Materials, 2015, Vol. 51, No. 2, pp. 152–157. © Pleiades Publishing, Ltd., 2015.
Original Russian Text © K.A. Petrovykh, A.A. Rempel, V.S. Kortov, E.A. Buntov, 2015, published in Neorganicheskie Materialy, 2015, Vol. 51, No. 2, pp. 193–198.

Sol–Gel Synthesis and Photoluminescence of Zn_2SiO_4:Mn Nanoparticles

K. A. Petrovykh[a, b], A. A. Rempel[a, b], V. S. Kortov[b], and E. A. Buntov[b]

[a] *Institute of Solid State Chemistry, Ural Branch, Russian Academy of Sciences, Pervomaiskaya ul. 91, Yekaterinburg, 620990 Russia*

[b] *Yeltsin Federal University, ul. Mira 19, Yekaterinburg, 620002 Russia*

e-mail: kspetrovykh@mail.ru

Received February 27, 2014

Abstract—Manganese-doped zinc orthosilicate (Zn_2SiO_4:Mn) nanoparticles have been prepared using a sol–gel process followed by annealing. The doping level was varied widely: from 0.1 to 10 at % Mn. The average particle size of the as-prepared material was 20 nm. With increasing annealing temperature, the particle size increased, reaching 150 nm as evaluated by X-ray diffraction. The photoluminescence intensity in the material was shown to depend significantly on the phase composition of the samples, the degree of their crystallinity, and the doping level.

DOI: 10.1134/S0020168515020156

INTRODUCTION

In recent years, nanoparticulate inorganic phosphors have been the subject of increasing attention as materials for modern displays, plasma display screens, and lighting devices. They are also potentially attractive for biological and medical applications. Nanophosphors offer a high quantum yield, improved adhesion to substrates, and enhanced radiation resistance in comparison with their microcrystalline analogues [1–3].

Zinc orthosilicate, Zn_2SiO_4 (willemite), is widely used as an excellent host for a variety of dopants. Doping with rare-earth and transition-metal ions (Mn^{2+}, Eu^{3+}, Ni^{2+}, and others) ensures high luminescence intensity in different parts of the visible range. Willemite is known to exist in several crystalline polymorphs. The most thermodynamically stable one is α-Zn_2SiO_4, whose structure is made up of $[SiO_4]^{4-}$ and $[ZnO_4]^{6-}$ tetrahedra. One of the most convenient dopants is manganese (Mn^{2+}). Since it is similar in ionic radius and oxidation state to Zn^{2+}, it readily substitutes on the Zn site, so manganese ions can be homogeneously distributed over the orthosilicate host. Thus, the most promise for practical application is offered by α-Zn_2SiO_4:Mn, which exhibits bright green luminescence under UV or electron beam excitation [4, 5].

Various processes for the preparation of Zn_2SiO_4:Mn have been described in the literature, for example, solid-state reaction, pulsed laser deposition, hydrothermal crystallization, and high-energy ball milling [6–8]. Each of these methods has its own benefits. Sol–gel processing offers a number of advantages: simple apparatus, low synthesis temperatures, molecular-scale homogeneity of the final product, and the possibility of producing multicomponent nanoparticulate phosphors [9, 10]. Moreover, this approach makes it possible to synthesize materials in a rather wide range of doping levels. One distinctive feature of the sol–gel synthesis of α-Zn_2SiO_4:Mn is that additional, high-temperature annealing is needed, which leads to an increase in the particle size of the material. At present, considerable attention is paid to the development of a sol–gel process for the preparation of a Zn_2SiO_4:Mn nanophosphor with controlled particle size and morphology [11–13].

In connection with this, the objectives of this work were to prepare Zn_2SiO_4:Mn by a sol–gel process and study the effect of annealing temperature, phase composition, and doping level on its photoluminescence (PL).

EXPERIMENTAL

The precursors used in the sol–gel synthesis of Zn_2SiO_4:Mn were zinc chloride ($ZnCl_2$), manganese chloride tetrahydrate ($MnCl_2 \cdot 4H_2O$), and tetraethyl orthosilicate (TEOS) ($Si(OC_2H_5)_4$). The synthesis method chosen allowed us to vary the Mn^{2+} dopant concentration over a wide range: from 0.1 to 10 at %. First, we prepared an aqueous solution of the metal chlorides and a water–alcohol solution of TEOS. To accelerate TEOS hydrolysis, we used hydrochloric acid as a catalyst. After the solutions were poured together, they were stirred on a magnetic stirrer for 1 h. The resultant sol was transparent, homogeneous, and

colorless to beige in color, depending on the doping level.

Gelation took place in air at room temperature. After homogenization of the gel throughout the beaker, the material was dried at a temperature of 75°C. As a result, we observed a considerable decrease in the volume of the gel (shrinkage). After drying, to remove physically bound water the gel was annealed at a temperature of 220°C for 2 h and took the form of dry powder.

To obtain crystalline α-Zn_2SiO_4:Mn, which offers the brightest luminescence, dry powders were annealed in air in the temperature range from 500 to 1200°C at 100°C intervals for 2 h at each temperature. To minimize the residual stress and prevent the formation of other willemite polymorphs, the samples were cooled to room temperature at a slow rate (were furnace-cooled).

The phase composition and crystallinity of the Zn_2SiO_4:Mn powders were evaluated by X-ray diffraction on a Shimadzu MAXIMA-X XRD-7000 diffractometer (Cu$K_{\alpha_{1,2}}$ radiation). The particle size and morphology were assessed by scanning electron microscopy (SEM) on a Zeiss Sigma VP. The average particle size (crystallite size) D_{cr} was determined from the observed broadening of X-ray diffraction peaks. Diffraction line profiles were fitted using the pseudo-Voigt function, a weighted superposition of a Gaussian and Lorentzian. The crystallite size D_{cr} was evaluated by the Williamson–Hall method [14], which allows one to separate the particle size and strain contributions to diffraction line broadening and quantitatively determine the crystallite size and lattice strain.

The effects of crystal structure and doping level on the PL of the material were investigated using a PerkinElmer Model LS55 spectrometer. PL spectra were measured in phosphorescence mode. The delay time was 1 ms, and the excitation wavelength was λ_{ex} = 250 nm. At doping levels under 1 at %, the monochromator slit widths were 10 (excitation) and 5 nm (emission). At Mn^{2+} concentrations of 5 at % and higher, the slit widths were 15 and 20 nm, respectively.

RESULTS AND DISCUSSION

The X-ray diffraction patterns in Fig. 1 illustrate the effect of annealing temperature on the crystallinity of the sample containing 1 at % Mn^{2+}. It is seen that the material remained amorphous at annealing temperatures of up to 600°C. After heat treatment at this temperature, we observed the first, weak diffraction peaks, which were assigned to willemite, α-Zn_2SiO_4 (PDF, no. 70-1235). In addition to the reflections from α-Zn_2SiO_4, we detected peaks of hexagonal zinc oxide (wurtzite structure) (PDF, no. 76-704). It is worth pointing out that that the X-ray diffraction patterns contained a diffuse halo corresponding to an amorphous phase, which only disappeared after annealing at a temperature above 1000°C. The intensity of the reflections from α-Zn_2SiO_4:Mn gradually increased with increasing annealing temperature, and that of the reflections from ZnO decreased considerably. At the same time, after heat treatment at 1200°C, we observed strong structural reflections from quartz, SiO_2 (PDF, no. 85-794). One possible reason for the formation of this phase is that TEOS hydrolyzes more slowly than zinc and manganese chlorides, which leads to the presence of silicon not combined with zinc. The rate of formation of the crystalline phase and the degree of crystallinity in the samples with other manganese concentrations are similar to those in the Zn_2SiO_4:Mn powder containing 1 at % Mn. Thus, the manganese content has no significant effect on the crystallization rate.

On the other hand, the phase composition of the samples was found to depend on Mn^{2+} concentration. At dopant concentrations of up to 5 at %, no diffraction peaks of crystalline manganese compounds were detected, even though the X-ray diffraction patterns contained reflections from ZnO and SiO_2 as impurity phases. Thus, it is reasonable to assume that the dopant ions were well dispersed over the lattice of the α-Zn_2SiO_4 host. At the same time, at dopant concentrations of 5 at % and above the X-ray diffraction patterns showed reflections from hetaerolite, $ZnMn_2O_4$ (PDF, no. 71-2499). At low annealing temperatures, the $ZnMn_2O_4$ phase prevailed, but with increasing annealing temperature its content gradually decreased, whereas the percentage of α-Zn_2SiO_4 increased. Like at lower manganese concentrations, after heat treatment at 1200°C we observed reflections from SiO_2 and weak reflections from ZnO. The formation of the impurity phase $ZnMn_2O_4$ may be due to the high dopant concentration in the material, as a result of which the dopant ions cannot uniformly dissolve in the host. Therefore, a longer annealing time is needed to better disperse manganese over α-Zn_2SiO_4. More detailed information about the crystalline phases identified in the material is presented in the table.

It is worth pointing out that the material begins to crystallize at temperatures lower than those in the synthesis of willemite via solid-state reaction. This feature was also pointed out previously by Tsai et al. [15] and El Ghoul et al. [16]. Possible reasons for this include the small particle size, ionic–molecular scale intermixing of the components, and the formation of homogeneous sol and then gel that already have Zn–O–Si bonds.

According to SEM data, the particle size of as-dried Zn_2SiO_4:Mn was about 20 nm. Raising the

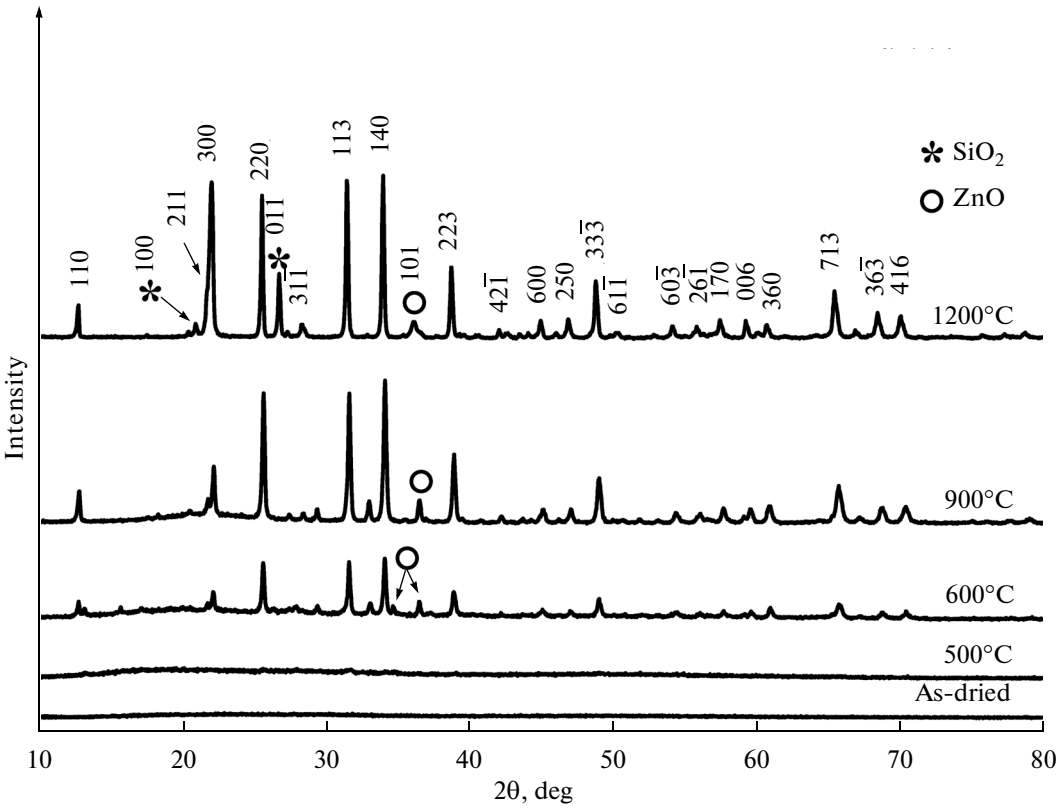

Fig. 1. X-ray diffraction patterns of sol–gel derived Zn_2SiO_4:Mn powder containing 1 at % Mn^{2+} after synthesis and annealing at various temperatures.

annealing temperature led to a systematic increase in the particle size of the material. For example, after heat treatment at a temperature above 1000°C the average grain size $D = D_{cr}$ was as large as 120 nm. The data in Fig. 2 illustrates the influence of annealing temperature on the particle size.

Figures 3 and 4 show the PL spectra of willemite samples for various annealing temperatures and Mn^{2+} dopant concentrations. In all instances, the peak emission wavelength is near 515 nm, which corresponds to the known electronic transition $^4T_1 \rightarrow {}^6A_1$ of the Mn^{2+} dispersed in the α-Zn_2SiO_4 lattice [17].

Figure 3 illustrates the effect of annealing temperature on the luminescence intensity in Zn_2SiO_4:Mn containing 1 at % Mn. It is seen that, with increasing annealing temperature, the PL intensity increases considerably. This is due to the improvement of the crystallinity of the material and the gradual increase in the percentage of α-willemite.

The annealing temperature and phase composition were found to have an intriguing effect on the PL of the samples doped with Mn^{2+} to 1 at % or more. In particular, after heat treatment at 1200°C the emission intensity was markedly lower in comparison with that at lower annealing temperatures (Fig. 4). The likely reason for this is that the samples contained little α-Zn_2SiO_4, whereas quartz and hetaerolite do not emit in the spectral region in question. The effect was particularly strong at a Mn^{2+} content of 10 at %: no PL was detected in the samples annealed at temperatures below 900°C.

The PL of the material was also influenced by the doping level. Increasing the Mn^{2+} concentration from 0.1 to 0.5 at % increased the emission intensity, whereas the intensity decreased considerably when the dopant concentration was increased from 5 to 10 at % (Fig. 4). Similar data were reported, for example, by Cho and Chang [5] and Tsai et al. [15], and were interpreted as the concentration quenching of luminescence, due to interaction between neighboring Mn^{2+} ions. Nevertheless, it is worth pointing out that there is currently no consensus as to the mechanism of this quenching. The spectral position and intensity of luminescence bands are known to depend on the crystalline environment of the dopant ion. In particular, the brightest 515-nm luminescence is ensured by the presence of MnO_4 tetrahedra in the structure of willemite. Increasing the doping level may lead to the formation of Mn pair centers substituting on nearest

Phase composition of sol–gel derived Zn_2SiO_4:Mn powders annealed at various temperatures

at % Mn^{2+}	Crystalline phases identified and their weight percentages		
	600°C	900°C	1200°C
0.1	α-Zn_2SiO_4, 96 ZnO, 4	α-Zn_2SiO_4, 99 ZnO, 1	α-Zn_2SiO_4, 90 SiO_2, 7.5 ZnO, 2.5
0.5	α-Zn_2SiO_4, 93 ZnO, 7	α-Zn_2SiO_4, 96.6 ZnO, 3.4	α-Zn_2SiO_4, 94.3 SiO_2, 3.5 ZnO, 2.2
1	α-Zn_2SiO_4, 94 ZnO, 6	α-Zn_2SiO_4, 96.4 ZnO, 3.6	α-Zn_2SiO_4, 82.5 SiO_2, 14.7 ZnO, 2.8
5	$ZnMn_2O_4$, 91 α-Zn_2SiO_4, 9	α-Zn_2SiO_4, 50.4 $ZnMn_2O_4$, 49.6	α-Zn_2SiO_4, 82.8 SiO_2, 8.7 $ZnMn_2O_4$, 7.4 ZnO, 1.1
10			$ZnMn_2O_4$, 46.5 SiO_2, 29.5 α-Zn_2SiO_4, 24

neighbor Zn sites [18]. Closely spaced dopant ions may also form Mn–O–Mn structures, which are known to exhibit no luminescence, as exemplified by manganese oxide. Concentration quenching was reported for a variety of doping hosts [17].

Moreover, it can be seen from the table that an increase in manganese concentration is accompanied by a sharp drop in the weight percentage of the α-Zn_2SiO_4:Mn phase. The resulting phases, which accumulate most of the Mn^{2+} ions in the composition of an alternative structure (hetaerolite) or as interstitial atoms (SiO_2) do not ensure crystal field symmetry characteristic of MnO_4 tetrahedra, which leads to a considerable reduction in 515-nm PL intensity. It seems likely that it is the combination of the above factors which is responsible for the nonmonotonic variation of the PL intensity with dopant concentration at Mn contents of 1 at % and higher.

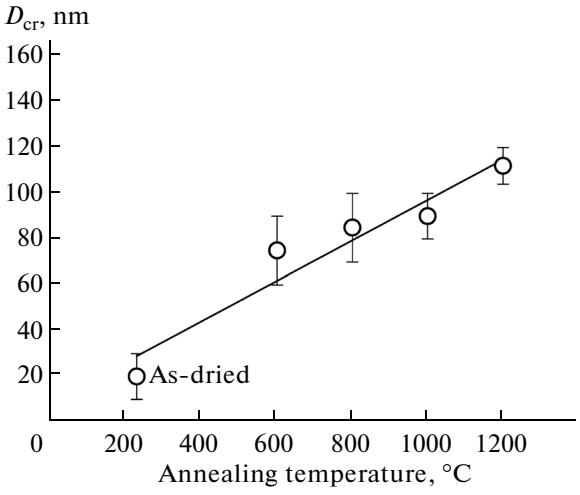

Fig. 2. Average crystallite size as a function of annealing temperature for the Zn_2SiO_4:Mn powder containing 1 at % Mn^{2+}.

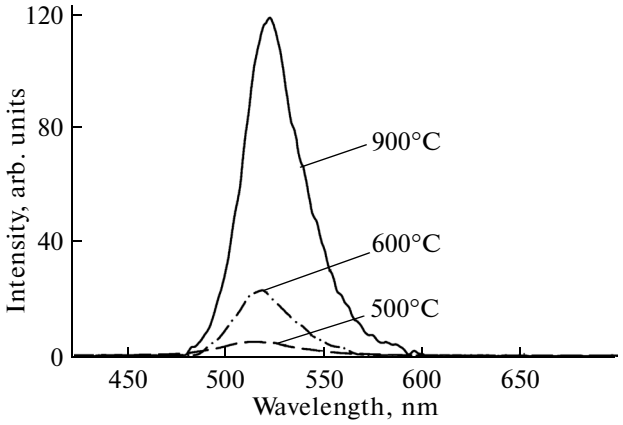

Fig. 3. PL spectra of Zn_2SiO_4:Mn powders containing 1 at % Mn^{2+} after annealing at different temperatures.

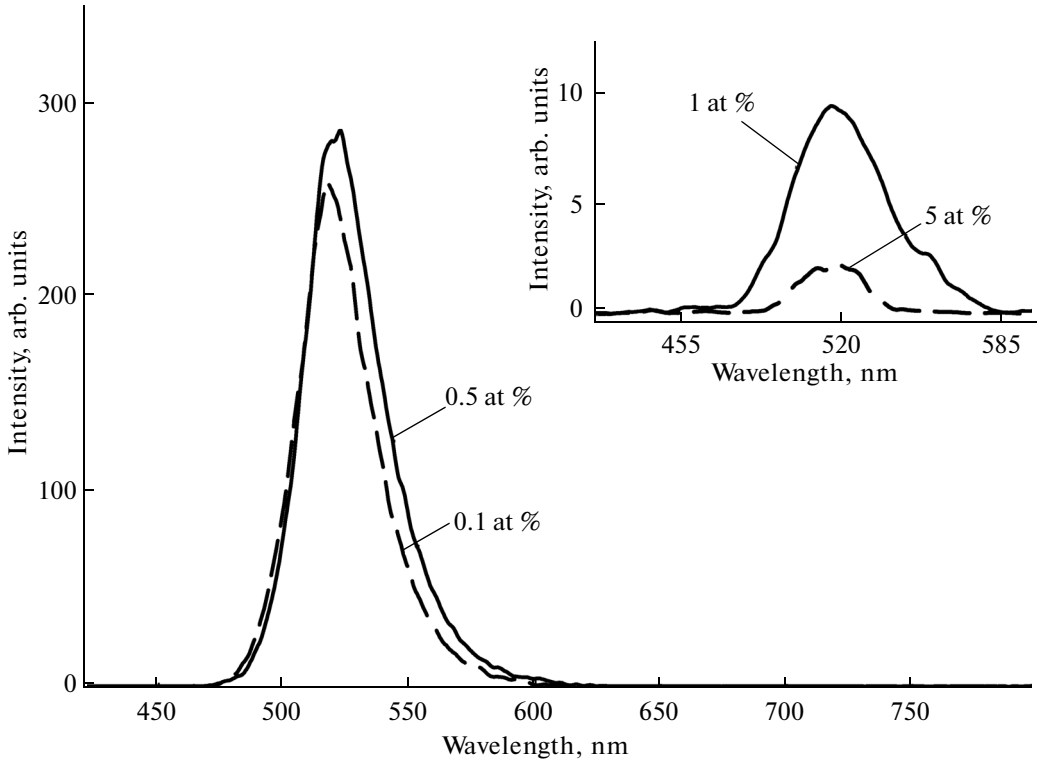

Fig. 4. Effect of Mn^{2+} dopant concentration on the PL spectrum of the Zn_2SiO_4:Mn powders annealed at 1200°C. The spectra in the main panel and inset differ in intensity scale because different monochromator slit widths were used.

CONCLUSIONS

Using a sol–gel process, we synthesized Zn_2SiO_4:Mn powders containing 0.1 to 10 at % Mn. The as-prepared material was amorphous, with an average particle size of 20 nm. Subsequent annealing in the temperature range from 500 to 1200°C resulted in crystallization, gave rise to PL, and increased the particle size to 150 nm. Analysis of X-ray diffraction data indicated that the material had a heterophase crystal structure and that the phase composition of the samples depended significantly on manganese concentration. In contrast, the degree of crystallinity of the material was independent of doping level but was influenced by the annealing temperature.

The synthesized Zn_2SiO_4:Mn nanophosphor exhibits green photoluminescence corresponding to α-willemite doped with manganese (Mn^{2+}). The PL depends significantly on the doping level and phase composition of the samples. The highest PL intensity is offered by the material containing 0.5 at % Mn^{2+}.

REFERENCES

1. Feldman, C., Jüstel, T., Ronda, C.R., and Schmidt, P.J., Inorganic luminescent materials: 100 years of research and application, *Adv. Funct. Mater.*, 2003, vol. 13, no. 7, pp. 511–516.
2. *Phosphor Handbook*, Yen, W.M., Shionoya, S., and Yamamoto, H., Eds., Boca Raton: CRC, 2006, 2nd ed.
3. Franz, K.A., Kehr, W.G., Adam, W., et al., Luminescent materials, in *Ulmann's Encyclopedia of Industrial Chemistry*, 2002, vol. A15, pp. 519–557.
4. Morell, A. and Khiati, N.El., Green phosphors for large plasma TV screens, *J. Electrochem. Soc.*, 1993, vol. 140, no. 7, pp. 2019–2022.
5. Cho, T.H. and Chang, H.J., Preparation and characterization of Zn_2SiO_4:Mn green phosphors, *Ceram. Int.*, 2003, vol. 29, pp. 611–618.
6. Takesue, M., et al., Thermal and chemical methods for producing zinc silicate (willemite), *Prog. Cryst. Growth Charact. Mater.*, 2009, vol. 55, pp. 98–124.
7. Petrovykh, K.A., Rempel, A.A., Kortov, V.S., et al., Disintegration of microcrystalline Zn_2SiO_4:Mn phosphor powder, *Inorg. Mater.*, 2013, vol. 49, no. 10, pp. 1019–1022.
8. Yan, J., Zhenguo, J., Junhua, X., et al., Fabrication and characterization of photoluminescent Mn-doped-Zn_2SiO_4 films deposited on silicon by pulsed laser deposition, *Thin Solid Films*, 2006, vol. 515, pp. 1877–1880.
9. Bakovets, V.V., Trushnikova, L.N., Korol'kov, I.V., et al., Synthesis of nanostructured luminophor Y_2O_3–Eu–Bi by the sol–gel method, *Russ. J. Gen. Chem.*, 2013, vol. 83, no. 1, pp. 1–9.
10. Cui, H., Zayat, M., and Levy, D., A general-assisted sol–gel route for the synthesis of metal oxide–silica

composites and silicates ultrafine particles, *J. Alloys Compd.*, 2009, vol. 474, pp. 292–296.

11. Yang, P., Lü, M.K., Song, C.F., et al., Preparation and characteristics of sol–gel derived Zn_2SiO_4 doped with Ni^{2+}, *Inorg. Chem. Commun.*, 2002, vol. 5, pp. 482–486.
12. Kong, D.Y., Yu, M., Lin, C.K., et al., Sol–gel synthesis and characterization of Zn_2SiO_4:Mn@SiO_2 spherical core–shell particles, *J. Electrochem. Soc.*, 2005, vol. 9, pp. 146–151.
13. El Mir, L., Amlouk, A., Barthou, C., et al., Synthesis and luminescence properties of $ZnO/Zn_2SiO_4/SiO_2$ composite based on nanosized zinc oxide-confined silica aerogels, *Phys. B* (Amsterdam, Neth.), 2007, vol. 388, pp. 412–417.
14. Williamson, G.K. and Hall, W.H., X-ray line broadening from filed aluminium and wolfram, *Act Metall.*, 1953, vol. 1, no. 1, pp. 22–31.
15. Tsai, M.-T., Wu, J.-M., Lu, Yu-F., and Chang, H.-C., Synthesis and luminescence characterization of manganese-activated willemite gel films, *Thin Solid Films*, 2011, vol. 520, pp. 1027–1033.
16. El Ghoul, J., Omri, K., El Mir, L., et al., Sol–gel synthesis and luminescent properties of SiO_2/Zn_2SiO_4 and SiO_2/Zn_2SiO_4:V composite materials, *J. Lumin.*, 2012, vol. 132, pp. 2288–2292.
17. Linwood, S.H. and Weyl, W.A., The fluorescence of manganese in glasses and crystals, *J. Opt. Soc. Am.*, 1942, vol. 32, pp. 443–453.
18. Robbins, D.J., Mendez, E.E., Giess, E.A., and Chang, I.F., Pairing effects in the luminescence spectrum of Zn_2SiO_4:Mn, *J. Electrochem. Soc.*, 1984, vol. 131, pp. 141–146.

Translated by O. Tsarev